Synthesis and Photophysical Properties of Some Benzoxazole and Benzothiazole Compounds

**Ying-Hung So,*,† Jeffrey M. Zaleski,‡ Cheryl Murlick,† and Ahmed Ellaboudy†**

The Dow Chemical Company, Central Research and Development, 1712 Building, Midland, Michigan 48674, and the Department of Chemistry, Michigan State University, East Lansing, Michigan 48824

Received September 21, 1995; Revised Manuscript Received January 15, 1996⊗

ABSTRACT: Several benzoxazole and benzothiazole compounds have been prepared and their extended configurations characterized by optical absorption and emission spectroscopy. In general, solutions of these compounds fluoresce strongly and exhibit emission spectral profiles which mirror their respective excitation spectra. One exception to this correlation results from a chromophore with a nonplanar ground state configuration which disrupts the extended π-network, promoting a strong hypsochromic shift of the absorption spectrum. The absorption, excitation, and emission spectra of these compounds also show a strong vibronic progression of ∼1300 cm^{-1} in accordance with the energy of ring-stretching modes for aromatic frameworks. This excited state molecular distortion is consistent with the $\pi\pi^*$ nature of the optical excitation. Also, the energy gap between excitation and emission 0−0 bands of these benzoxazole and benzothiazole compounds and their polymeric forms are strongly influenced by the minimum allowed intermolecular space. In dilute solutions or for structures with bulky substituents, only small energy differences are observed between excitation and fluorescence 0−0 bands. In contrast, solid state samples devoid of side groups exhibit significantly larger energetic displacements accompanied by a pronounced broadening of both excitation and emission spectral profiles. These results suggest that strong intermolecular π-stacking interactions occur for the planar benzoxazoles and benzothiazoles in the solid state. Excited state lifetime decay measurements for PBO model compounds in toluene are monoexponential with essentially identical lifetimes under evacuated and standard pressure conditions. In the solid state, PBO and PBT model compounds exhibit biexponential luminescence decay lifetimes which were also not significantly affected by the presence of O$_2$. Fibers of PBO and PBT revealed three oxygen independent, but wavelength dependent emitting species. The presence of only one emitting species for these benzoxazole compounds in solution, compared with their multiexponential lifetime behavior in the solid state, further supports strong π-interactions between these molecules in the solid state. This molecular configuration permits benzoxazole and benzothiazole compounds to undergo photoinduced electron transfer in the solid state, which in the presence of oxygen leads to the generation of superoxide.

Introduction

Poly(benzo[1,2-*d*:5,4-*d′*]bisoxazole-2,6-diyl-1,4-phenylene) (*cis*-PBO) and poly(benzo[1,2-*d*:4,5-*d′*]bisthiazole-2,6-diyl-1,4-phenylene) (*trans*-PBT) have unique extended rigid-rod-like configurations. These polymers have excellent thermal and oxidative stability and good hydrolytic and solvent resistance. Fibers of these polymers have extremely high tensile strength and tensile modulus. The synthesis, process, and properties of these polymers have been actively pursued.[1−4]

cis-**PBO**   trans-**PBT**
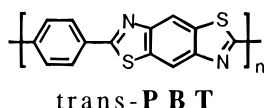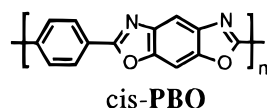
Photostability is an important issue for outdoor applications of a polymer. Thin Kelvar aramid fiber fabrics lose about half of their tensile strength if exposed directly to Florida sunlight for an extended period.[5] PBT fiber, on the other hand, has excellent ultraviolet light stability. Long exposure to ultraviolet light affects the fiber strength only slightly.[6]

Although PBT and PBO can potentially be very important commercial polymers,[7] only a modest number of studies addressing the photophysical and photochemi-

cal properties of benzothiazole and benzoxazole have been reported.[8−12] It is well established that the benzoxazole group has a considerable chromophoric effect on the fluorescence of conjugated systems because it enhances the emission quantum yield via a decrease in the nonradiative decay rate constant.[8] The chromophoric effect of the benzoxazole group has been used in industrial fluorescers such as optical brighteners, organic scintillators, and laser dyes.[9,13−15] The latter applications have shown that 2,6-diphenylbenzo[1,2-*d*:4,5-*d′*]bisoxazole (**1**) exhibits high photostability in ethanol/dioxane solution.[9]

1
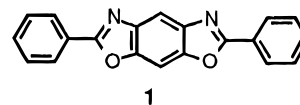
The advantageous physical properties of these polymeric materials, coupled with their interesting photophysical features, have prompted studies concerned with identifying the nature of their highly luminescent excited state. These planar polymeric materials have been shown to have closely packed π-conjugated structures capable of interchain excimer as well as charge transfer complex (exciplex) formation.[10]

In this work, the preparation and photophysical characterization of several benzoxazole and benzothiazole model compounds are described. Compounds possessing more than one benzobisoxazole unit dissolve only in strong acids which induces protonation of the nitrogens in the heterocyclic rings. Two benzoxazole

† The Dow Chemical Company.
‡ Michigan State University. Present address: Department of Chemistry, Stanford University, Stanford, CA 94305.
⊗ Abstract published in *Advance ACS Abstracts,* March 1, 1996.

derivatives with aliphatic side chains were prepared to allow studies of extended benzoxazoles in the *nonprotonated state*. This extended architecture can induce nonplanar structures due to steric hindrance. The UV–vis absorption spectra, excitation and emission spectra, and excited state lifetime decay measurements of several benzoxazole and benzothiazole compounds are reported. ESR spectroscopy studies investigating photoinduced electron transfer reactions with molecular oxygen are also described.

Results and Discussion

I. Synthesis of Benzoxazole and Benzothiazole Compounds.

2,2′-(1,4-Phenylene)bis(5-amino-6-benzoxazolol) and its phosphate esters (**2**) were isolated from the product mixture of excess 1,3-diamino-4,6-dihydroxybenzene dihydrochloride (DADHB) with terephthalic acid (TA). Reaction of **2** with benzoic acid produced 2,2′-(1,4-phenylene)bis(6-phenylbenzo[1,2-*d*:5,4-*d′*]bisoxazole) (**3**) and with 3,5-di-*tert*-butylbenzoic acid generated 2,2′-(1,4-phenylene)bis[6-[3,5-bis(1,1-dimethylethyl)phenyl]benzo[1,2-*d*:5,4-*d′*]bisoxazole] (**4**).

**2** X = H or OP(O)₂OH

3 R = H
4 R = t-Butyl
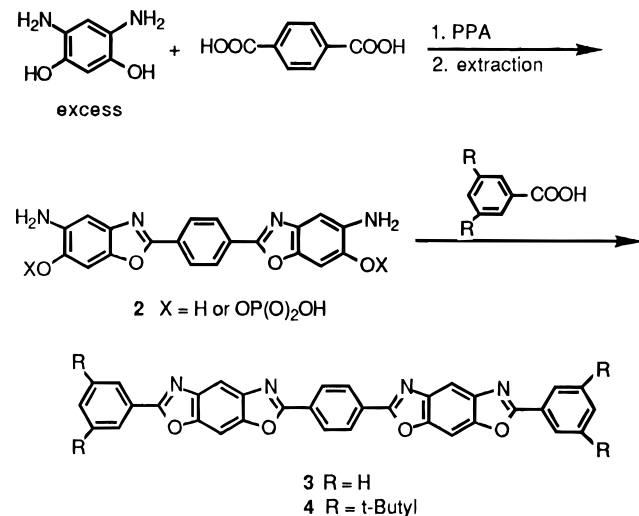
2,2′-(2,3,5,6-Tetramethyl-1,4-phenylene)bis(5-amino-6-benzoxazolol) and its phosphate esters (**5**) were prepared by the reaction of excess DADHB with 2,3,5,6-tetramethylterephthalic acid followed by extraction with 1 N NaOH solution. Reaction of **5** with 4-heptylbenzoic acid generated 2,2′-(2,3,5,6-tetramethyl-1,4-phenylene)-bis[6-(4-heptylphenyl)benzo[1,2-*d*:5,4-*d′*]bisoxazole] (**6**).

**5** X = H or OP(O)₂OH

6
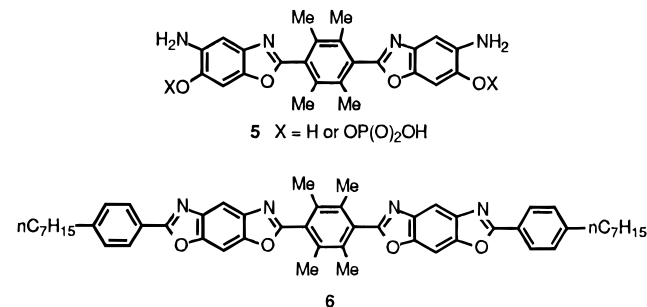
4-Bromobenzoic acid reacted with *o*-aminophenol to generate 2-(4-bromophenyl)benzoxazole (**7**) which was

converted to 4-(2-benzoxazolyl)benzoic acid (**8**) by quenching the Grignard product of **7** with CO_2. DADHB reacted with **8** in PPA to produce 2,6-bis[4-(2-benzoxazolyl)phenyl]benzo[1,2-*d*:5,4-*d′*]bisoxazole (**9**).
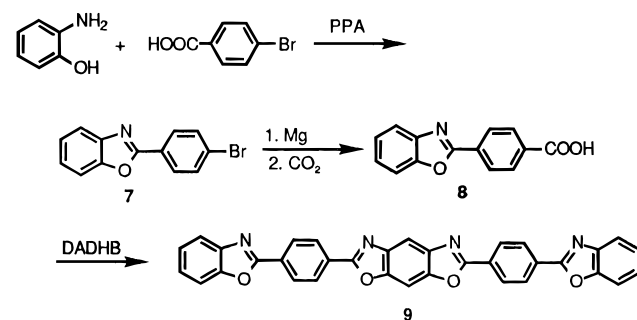

Reaction of *o*-aminothiophenol with 4-cyanobenozyl chloride produced 4-(2-benzothiazolyl)benzonitrile (**10**) which was converted to 4-(2-benzothiazolyl)benzoic acid (**11**). DADTB condensed with **11** in PPA to produce 2,6-bis[4-(2-benzothiazolyl)phenyl]benzo[1,2-*d*:4,5-*d′*]bisthiazole (**12**).
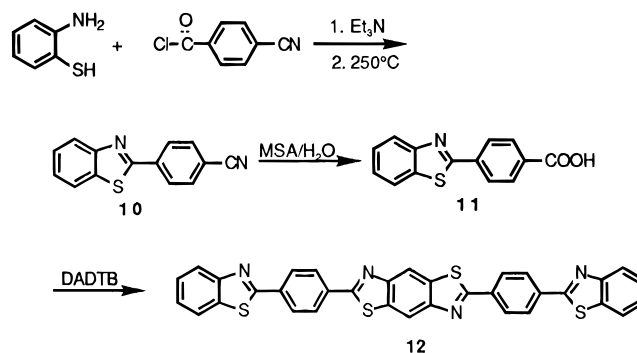
II. Protonation of Benzoxazole in Strong Acids

Figures 1 and 2 show the proton and carbon-13 NMR spectra of 2,6-bis(4-*tert*-butylphenyl)benzo[1,2-*d*:4,5-*d′*]-bisoxazole (**13**) in CDCl₃ and in methanesulfonic acid (MSA) with tentative peak assignments. Dramatically different resonance energies are observed for the benzobisoxazole ring protons and carbon atoms when spectra were recorded in deuterated chloroform and MSA, suggesting protonation of the heterocyclic ring nitrogens in this strongly acidic medium.

1 3
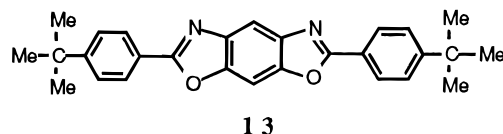
III. Absorption Spectroscopy.

Figure 3 shows the UV absorption spectra of **1** and **4** in chloroform and MSA. The absorption profile of both compounds in chloroform reveals a strong vibronic progression of $\sim$1300 cm^{-1} in accordance with the energy of ring-stretching modes for aromatic frameworks.[16] This excited state molecular distortion is consistent with the $\pi\pi^*$ nature of the optical excitation.[8] A significant red shift of the lowest energy absorption band and a pronounced broadening of the vibronic fine structure are observed when these compounds are dissolved in MSA. Although the optical spectra of **4** and thin layers of
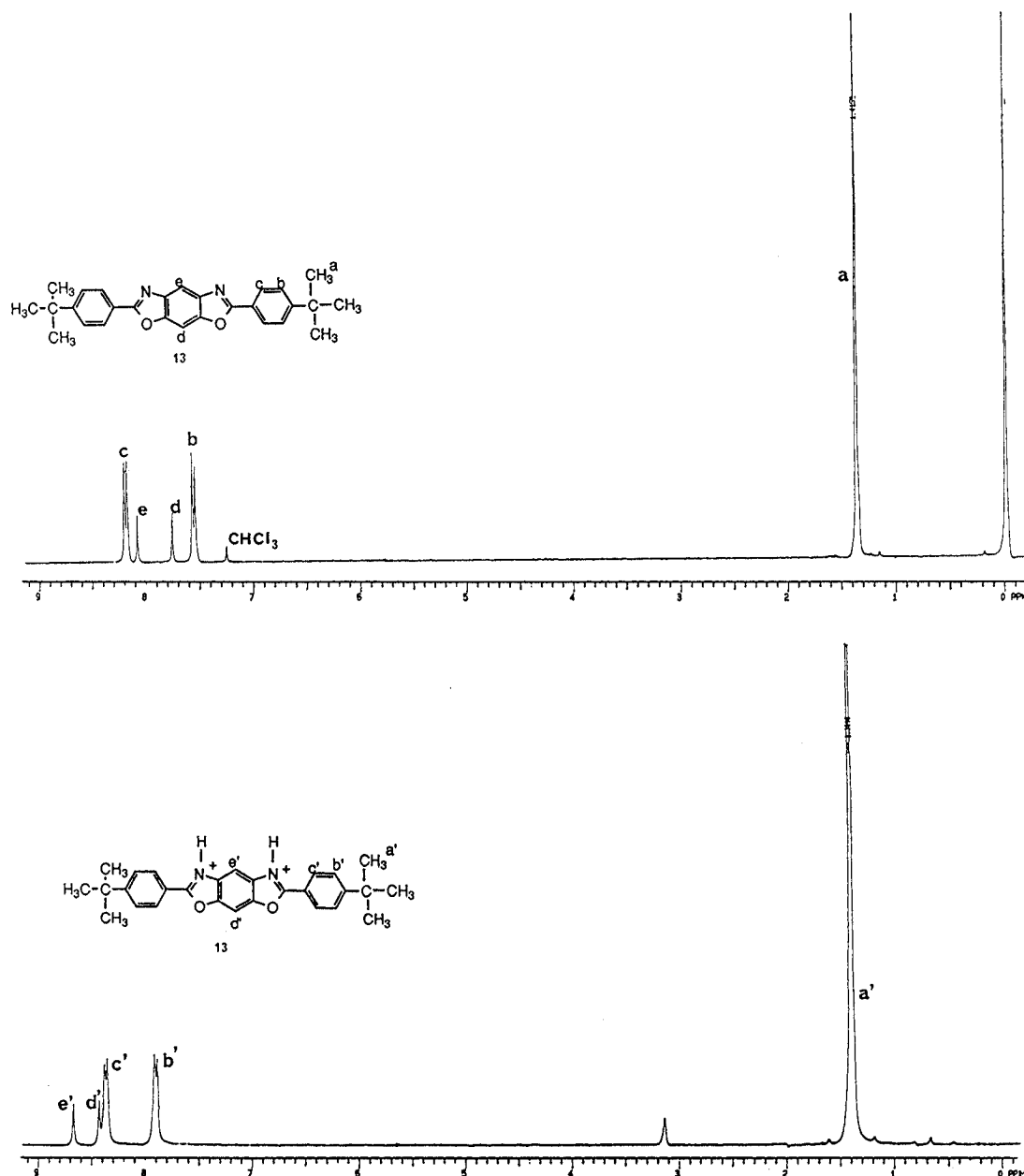
Figure 1. (Top) ^{1}H NMR spectra of **13** in CDCl$_3$ with tentative peak assignments. (Bottom) ^{1}H NMR spectra of **13** in MSA with tentative peak assignments.

sublimed **3** and **9** reveal no absorption bands in the visible region, consistent with their lack of detectable color, they instantaneously turn yellow upon contact with MSA or trifluoroacetic acid (TFA) due to protonation of the aromatic nitrogens. The UV−vis absorption spectra of **9** and **12** in MSA show characteristics similar to **1** and **4** and are shown in Figure 4. The red shift of the absorption profile of **12** relative to **9** is consistent with the greater electron-donating ability of the heterocyclic sulfur atoms. Figure 4 also show the UV spectra of PBO and PBT in MSA and a PBO film.

The absorption properties of **6**, **1**, and **4** in different solvents and **3, 9, 12,** PBO, and PBT in MSA are summarized in Table 1. The hypsochromic shift of the absorption spectrum of **6** suggests the chromophore is in a nonplanar conformation due to the steric hindrance introduced by the ortho and ortho′ methyl groups of the central phenyl ring.[9,17]

Photolysis of polymers in air and nitrogen often shows a variety of results,[18−20] with some polymers undergoing photooxidative reactions through the formation of charge transfer complexes with molecular oxygen.[21] Compound **4** was used to study the possible formation of charge transfer complexes between oxygen and PBO model compounds *in solution* because of its solubility in organic solvents. A toluene solution of **4** in a quartz UV cell was bubbled with nitrogen or oxygen gas and then capped right before UV spectra were recorded. The two spectra were identical. The excitation spectrum under 94.7 psi oxygen showed no additional charge transfer bands. Therefore, we conclude that charge transfer complex formation between **4** and molecular oxygen in solution does not occur.

IV. Excitation and Emission Spectra of Benzoxazole and Benzothiazole Compounds and Polymers. Solutions of benzoxazole and benzothiazole compounds in chloroform, toluene, or MSA fluoresce strongly and exhibit emission spectral profiles which mirror their respective excitation spectra with the exception of compound **6**. The excitation and emission spectra of **6** and **4** in chloroform are shown in Figure 5. While the excitation and emission profiles of **4** have
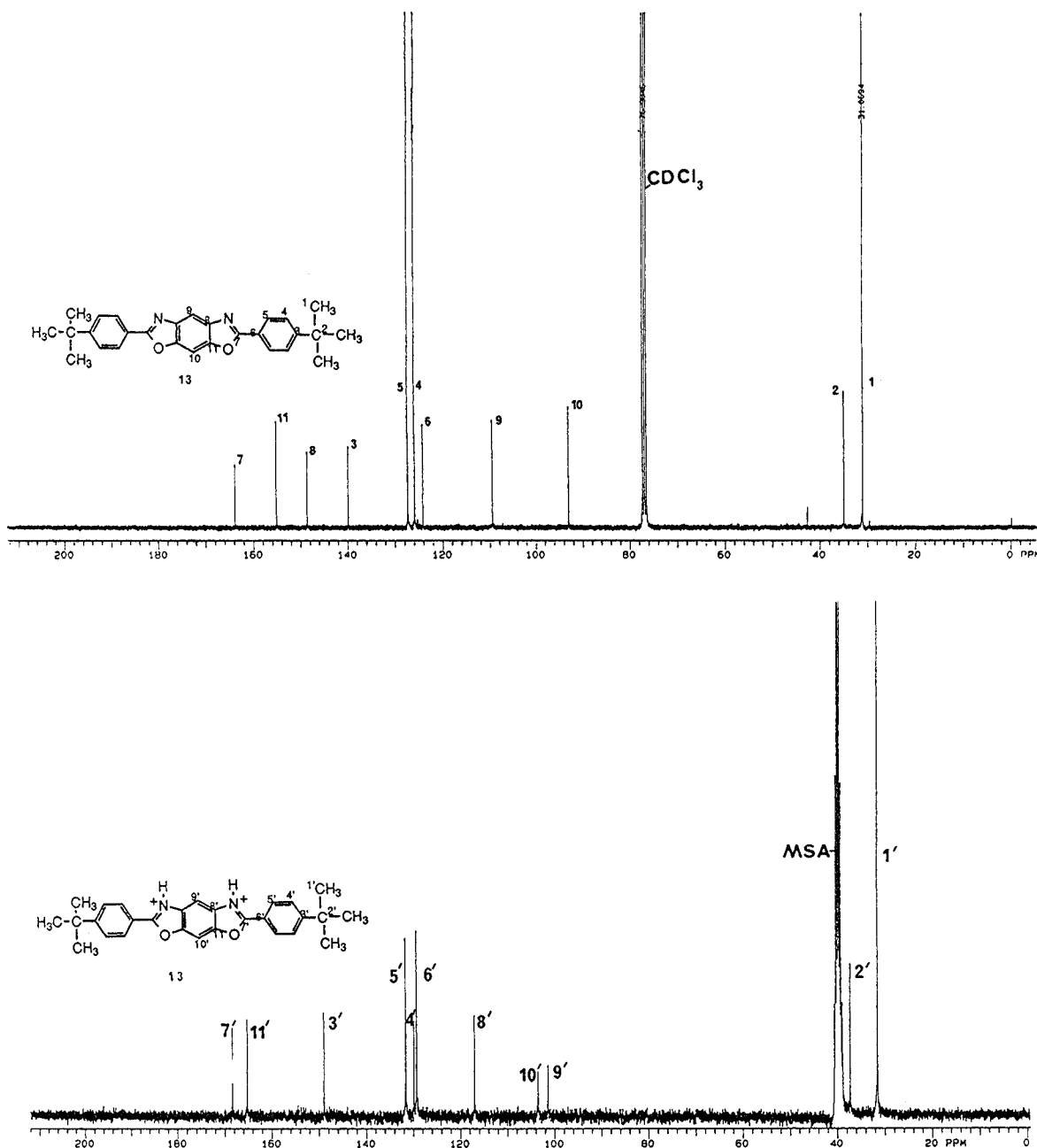
Figure 2. (Top) ^{13}C NMR spectra of **13** in CDCl$_3$ with tentative peak assignments. (Bottom) ^{13}C NMR spectra of **13** in MSA with tentative peak assignments.
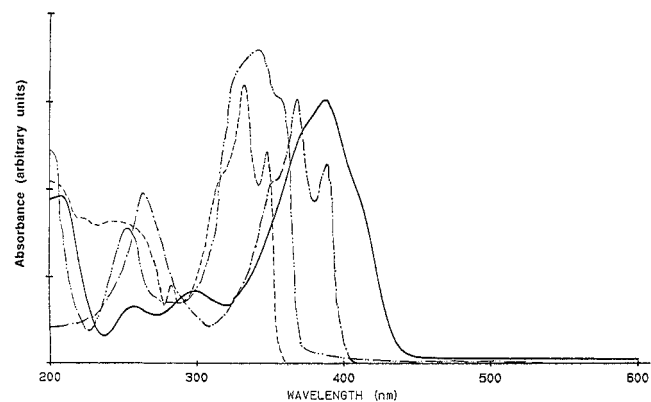
Figure 3. UV spectra of **1** and **4** in CHCl$_3$ and MSA: **1** in CHCl$_3$ (- - -), **1** in MSA (−··−), **4** in CHCl$_3$ (−·−), **4** in MSA (−).

Figure 4. UV spectra of **9** (- - -), **12** (−), PBO (−··−), and PBT (−···−) in MSA and a PBO film (−·−).

similar characteristics to other benzoxazole and benzothiazole compounds, the emission spectrum of **6** does

not exhibit the discrete vibronic features observed in the excitation spectrum. This is presumably due to a

Figure 5. Excitation and emission spectra of **4** (—, emission 425 nm, excited at 375 nm) and **6** (- - -, emission 400 nm, excited at 320 nm) in CHCl$_3$.

Figure 6. Excitation and emission spectra of **9** (—, emission 450 nm, excited at 380 nm) and **12** (- - -, emission 470 nm, excited at 400 nm) in MSA.

Table 1. Absorption Data of Some PBO Model Compounds

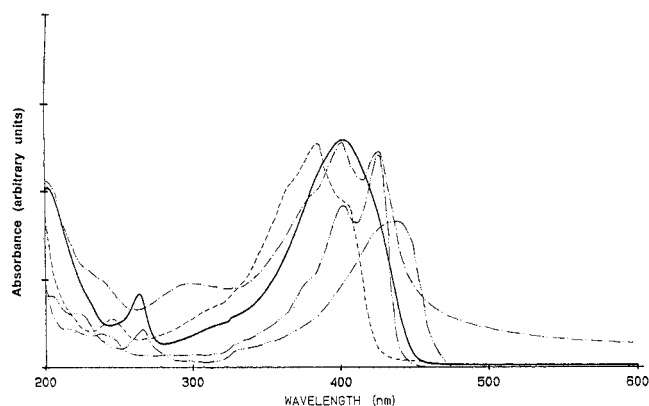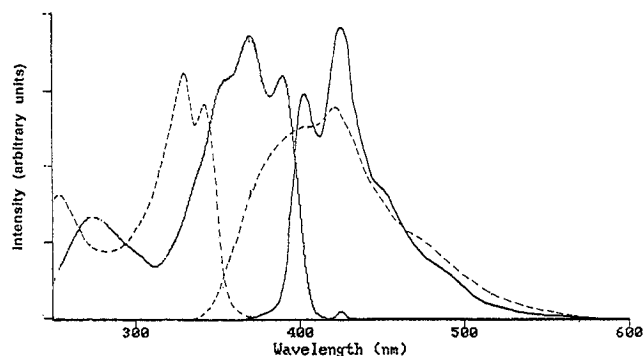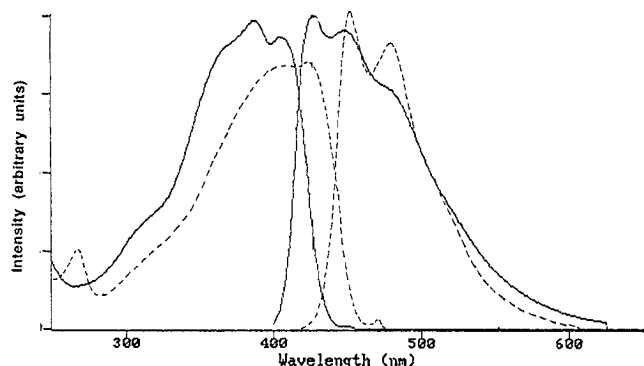| compd	solvent	0−0 band, nm	λ_{max}, nm	$\epsilon_{max} \times 10^{-4}$
6	chloroform	333	319	7.0
	MSA	360 shoulder	344	9.8
1	chloroform	349	334	3.0
	toluene	347	331	3.5
	CCl$_4$	350	333	3.0
	acetonitrile	347	332	3.0
	MSA	358	342	4.7
4	chloroform	391	371	7.6
	toluene	388	368	7.0
	MSA	414 shoulder	388	6.4
3	MSA	405	383	6.3
9	MSA	405	383	6.9
12	MSA		402	7.0
PBO film		426	402	
PBO	MSA		429	7.1
PBT	MSA		442	7.1

low barrier to free rotation in the $^1(\pi\pi^*)$ excited state induced by the nonplanar structure of the ground state molecule. Figure 6 shows the excitation and emission spectra of **9** and **12** in MSA. The enhanced broadening of the spectral features for these compounds is similar to that observed in the absorption spectra of **3** and **4** (*vide infra*) in this solvent.

Figure 7 shows the excitation and emission spectra of **1** in toluene and in the solid state, and Figure 8 shows those of **3**, **4**, and **6** in the solid state. Excitation and emission spectra of **9**, **12**, PBO, and PBT in the solid state are similar to that of **3** in that each displays a large difference between excitation 0−0 bands and fluorescence 0−0 bands (Stokes' shifts) which are listed in Table 2. The excitation and emission spectra of PBO and PBT fibers are shown in Figure 9.

Because compounds **3**, **9**, and **12** are not soluble in organic solvents, only solid state and MSA solution data
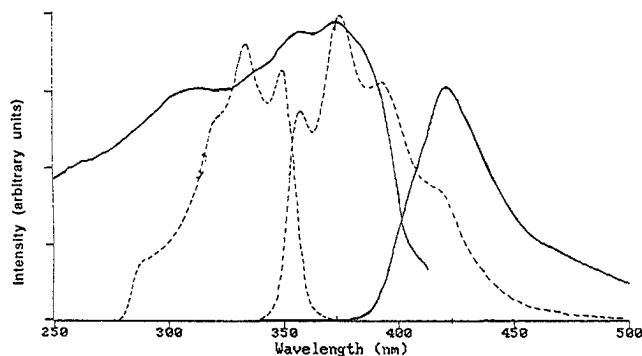

Figure 7. Excitation and emission spectra of **1** in toluene (- - -, emission 420 nm, excited at 320 nm) and in solid state (—, emission 420 nm, excited at 320 nm).
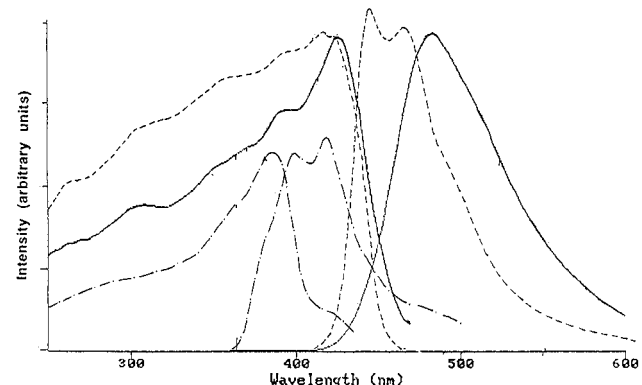

Figure 8. Soild state excitation and emission spectra of **3** (—, emission 484 nm, excited at 350 nm), **4** (- - -, emission 480 nm, excited at 360 nm), and **6** (−·−, emission 450 nm, excited at 320 nm).

Table 2. Excitation and Emission 0−0 Bands of Some PBZ^a Model Compounds and Polymers

compd	excitation 0−0 band, nm	emission 0−0 band, nm	Dl
1 solid state	373	422	49
1 in toluene^b	349	356	7
3 solid state	426	484	58
4 solid state	425	446	21
4 in toluene^b	396	408	12
6 solid state	387	400	13
6 in toluene^c	346		
9 solid state	431	491	60
9 in MSA	409	426	17
12 solid state	472	522	50
12 in MSA	424	452	28
PBO fiber	458	522	64
PBT fiber	561	613	52

^{a} PBZ stands for PBO and PBT. ^{b} Concentration was 3×10^{-5} M of **1**, **4**, or **6** in toluene. ^{c} Excitation and emission are not mirror images of each other.

of these chromophores were obtained. Data from compounds in MSA solutions should be interpreted with caution because the molecules are protonated.

The planar structures of compounds **1**, **3**, **9**, and **12** suggest that in the solid state molecules may orient in a π-stacked configuration while those that are nonplanar are less likely to exist in this conformation. The large Stokes shifts observed for planar model compounds in the solid state are also present in the excitation/emission spectra of PBO and PBT fibers, suggesting a similar molecular architecture. In contrast, interaction of an excited **4** molecule with its neighboring molecules is hindered by its four *tert*-butyl groups, and consequently a small Stokes shift is observed for **4** in the solid state. This is also true for **6**,
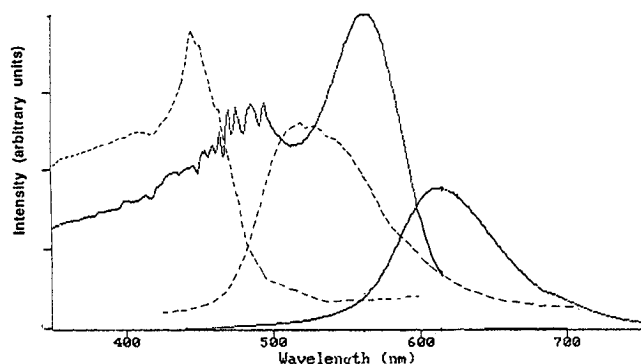
Figure 9. Excitation and emission spectra of PBO fiber (- - -, emission 520 nm, excited at 400 nm) and PBT fiber (—, emission 620 nm, excited at 420 nm).

Table 3. Lifetime Results for PBZ Model Compounds

sample	$\tau 1$, ns (%)	$\tau 2$, ns (%)	λ_{det}, nm
1E in toluene	1.25 (100)		400
1A in toluene	1.17 (100)		400
1E solid state	1.95 (69.95)	4.16 (30.05)	400
1A solid state	2.10 (61.45)	3.83 (38.55)	400
4E in toluene	1.07 (100)		400
4A in toluene	1.03 (100)		400
4E solid state	0.72 (29.34)	2.10 (70.66)	450
4A solid state	0.66 (42.32)	1.43 (57.68)	450
3E solid state	0.93 (43.10)	1.80 (56.90)	450
3A solid state	0.81 (43.63)	1.87 (56.37)	450
3A solid state		1.98[a]	400
9E solid state	0.66 (25.23)	2.69 (74.77)	450
9A solid state	0.52 (18.02)	2.35 (81.98)	450
12E solid state	1.22 (42.01)	2.26 (57.99)	500
12A solid atate	1.12 (43.76)	2.26 (56.24)	500

[a] Only 200 counts were obtained.

Table 4. Lifetime Decays for PBO and PBT Fibers

sample	$\tau 1$, ns (%)	$\tau 2$, ns (%)	$\tau 3$, ns (%)	λ_{det} (nm)
PBOE	0.05 (22.81)	0.22 (36.88)	0.79 (40.31)	450
PBOE	0.06 (19.97)	0.21 (57.15)	0.65 (22.89)	500
PBOE	0.08 (14.45)	0.28 (49.64)	1.48 (35.92)	550
PBOE	0.09 (9.50)	0.33 (36.93)	1.42 (53.57)	600
PBOE	0.08 (2.91)	0.32 (28.66)	1.49 (68.44)	650
PBOA	0.05 (15.51)	0.21 (63.62)	0.80 (20.87)	500
PBOA	0.07 (6.34)	0.29 (39.86)	1.41 (53.80)	600
PBTE			1.13[a]	500
PBTE	0.10 (6.89)	0.43 (31.15)	1.59 (61.96)	600
PBTA	0.08 (4.56)	0.38 (30.85)	1.55 (64.59)	600

[a] Only 200 counts were obtained.

which has a nonplanar structure due to the four methyl groups of the central phenyl ring.

Since the likelihood of intermolecular π-stacking is low in dilute solution, investigation of the spectral features of PBO and PBT model compounds under these conditions can be used to verify the presence of intermolecular interactions in the solid state. This correlation is indeed observed for a 3×10^{-5} M solution of **1** which shows a significantly smaller Stokes shift in solution than in the solid state. These results suggest that strong π-interactions exist between an excited benzoxazole molecule and the surrounding benzoxazole molecules in the solid state. This intermolecular interaction is responsible for the different photochemical behavior of these benzoxazoles in the solid state and in solution.[22]

V. Luminescence Lifetime Measurements. Tables 3 and 4 show the results of luminescence lifetime measurements of PBO and PBT model compounds and for PBO and PBT fibers, respectively. For sample identification, either "A" or "E" is appended to the sample name to represent lifetime measurements accomplished in air or in vacuum, respectively. All of the experiments were performed with 308 nm excitation into the $^1(\pi\pi^*)$ absorption manifold of the benzoxazole or benzothiazole chromophore. The detection wavelength for the model compounds was varied to achieve optimum luminescence intensity. For the model compounds, the only wavelength dependence study was performed with **3**A at 400 nm and 450 nm. For the PBO fiber, a complete wavelength dependence from 450 nm to 650 nm for the evacuated sample was carried out.

The luminescence decay for **1** in toluene is monoexponential under evacuated and standard pressure conditions possessing a lifetime of approximately 1.2 ns, which is typical of $^1(\pi\pi^*)$ states of aromatic systems and similar to those observed for benzoxazole and benzthiazole compounds previously.[8] The solid state samples, however, have biexponential decays with lifetimes of approximately 2.0 and 4.0 ns (Figure 10).

Similarly, lifetime decays for **4** in toluene are monoexponential and essentially oxygen independent. Compound **4** in the solid state may possess some photoreactivity with oxygen since the presence of O_2 induces a slight decrease in the lifetime of both components and a corresponding shift in the relative weights of the individual exponential functions. Although this is a measurable difference, it is not a large effect, presumably due to kinetic barriers to reactivity in the solid state.

For **3**E and **3**A with detection at 450 nm, the biexponential fits are very similar and show little, if any, effects of oxygen quenching, consistent with the $^1(\pi\pi^*)$ nature of the emitting state. For **3**A with detection at 400 nm, only 200 counts were obtained; however, the monoexponential lifetime is similar to the longer component of the biexponential analysis, and therefore, lifetime decays of **3**A are not strongly wavelength dependent.

The decays also appear to be very similar for samples **9**E and **9**A with detection at 450 nm and are comprised primarily of a ∼2.5 ns component (∼78%). The presence of oxygen does not significantly affect the lifetime. Samples **12**E and **12**A with detection at 500 nm are virtually identical with two components of similar lifetime.

In general, decay lifetimes of **1** and **4** in solution and the short life component of all benzoxazole and benzothiazole compounds in the solid state are similar to those observed directly by Güsten *et al.*[9] as well as those calculated by Reiser *et al.* on the basis of fluorescence quantum yield measurements.[8] Although the origin of the monoexponential lifetime components for these conjugated benzoxazoles is straightforward, those observed for compounds in the solid state are less clear. The electronic structural description of the singlet and triplet excited state manifolds put forth by Reiser *et al.* accounts for the enhancement in the fluorescence quantum yield and the excited state decay kinetics for compounds containing the benzoxazole chromophore in solution. However, the biexponentiality of the fluorescence decay for these compounds in the solid state, coupled with the excitation and emission spectral broadening and larger Stokes' shift compared to dilute solutions, suggests that the components with longer lifetimes in the solid state result from excimer formation as observed by Jenekhe and co-workers.[10]
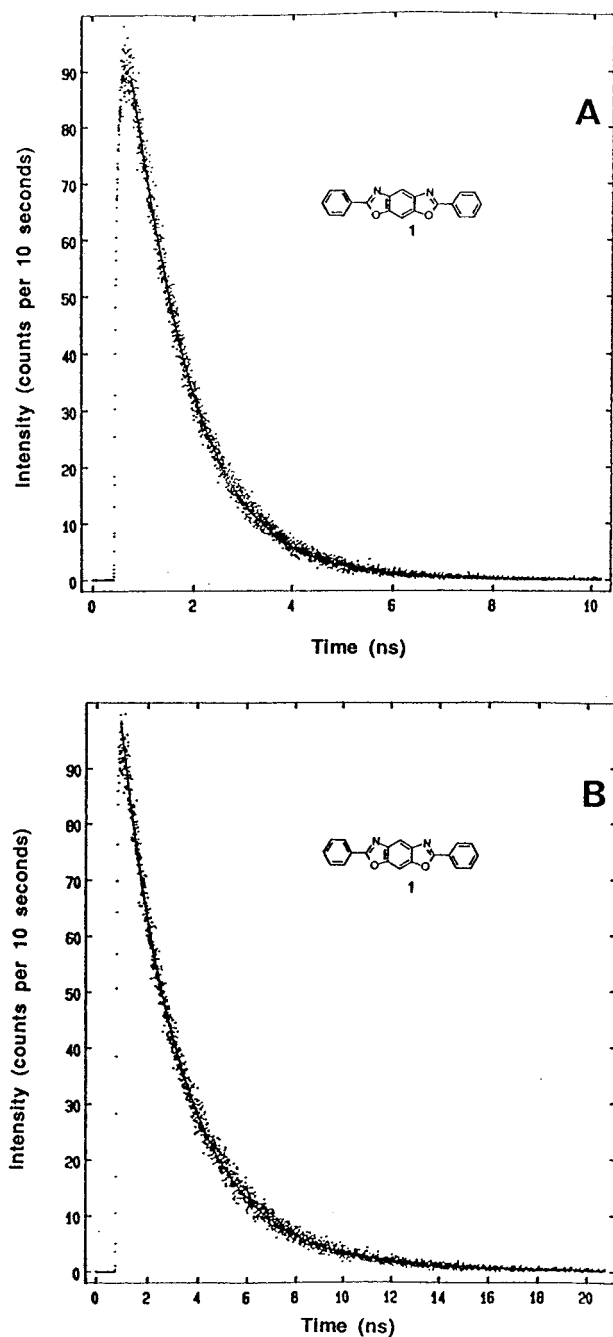
Figure 10. Fluorescence decay of **1** in toluene (air, A) and in solid state (air, B).

The luminescence lifetime decays for PBO and PBT fibers are given in Table 4. Analysis of PBO fiber luminescence decays obtained between 450 and 650 nm required the use of a three-term fit to converge. In many cases, the third component is significant (about 15−20%). The decays have been plotted with the instrument response function (FWHM ~ 50 ps) but were fit without deconvolution because the lifetime of the long-lived species was unchanged while that of the middle component displayed only small variations in the lifetime upon deconvolution analysis. In the range 450−500 nm the lifetimes are similar but the relative percentage of the longer components changes dramatically. Fluorescence decays obtained between 550 and 650 nm show a marked increase in the lifetime of the long-lived species accompanied by an increase in the relative contribution from that component to the ob-

served luminescence. Also, the percentage of short component begins to vanish, making the overall decay curve more genuinely biexponential. This type of behavior results from multiple emission bands which overlap through the visible spectrum. The presence of multiple emitting species in the PBOE fiber can best be attributed to excimer and charge transfer complex formation between closely spaced chromophores in the solid state, consistent with the large Stokes' shift and spectral broadening observed in the excitation and emission spectra. In addition, no real differences in the luminescence lifetime components of the PBO fiber are observed for samples measured in the presence of oxygen.

PBT fiber samples have similar lifetime decay curves when obtained under evacuated or standard pressure conditions. The decay curves were fit with a three-term exponential function in order to minimize the residuals, but the third component is relatively small. The PBT fiber luminescence lifetime obtained at 500 nm (200 counts) was underdetermined and difficult to fit to the same function. Therefore, the lifetime was extracted from a monoexponential fit which gave a value consistent with the three-term fits.

VI. Investigation of Possible PBO Excimer Formation in Solution. Excimer formation has been shown to occur in many organic systems[23] as well as in polymeric forms of poly(phenylene oxide),[19,20] PBO, and PBT.[10] Such complexes exist only in the excited state, and their formation is often accompanied by the appearance of a new emission at longer wavelengths, the intensity of which increases with concentration.[23]

A concentration dependence of the emission spectrum of **1** in chloroform was performed from 1.9×10^{-3} to 1.8×10^{-7} M. The observed spectral profiles were identical over this concentration range with no new emission bands detected. Above 2.5×10^{-5} M, inner-filter effects begin to perturb the emission spectrum of the solution.[24] No excimer formation of **1** in chloroform was observed up to this limiting concentration.

VII. Photolysis of Benzoxazole and Benzothiazole Compounds in the Solid State. The fact that only one emitting species was observed for **1** and **4** in solution whereas in the solid state these benzoaxzoles exhibit biexponential luminescence decay curves suggests that π-stacking intermolecular interactions are observed in the solid state. Because different results are obtained when these solid state benzoxazole compounds are photolyzed in solution versus the solid state, π-stacking interactions must enhance the photochemistry of these systems.[22] Together with the effect of these intermolecular interactions on the excitation and emission spectra of these benzoxazole and benzothiazole compounds, our results indicate excimer formation when PBO derivatives are photolyzed in the solid state, similar to that shown by Jenekhe and co-workers.[10] In general, excimer fluorescence is considered to be operative when the molecular components adopt a sandwich configuration with an interplanar distance of 3.0−3.6 Å and when both exciton and charge-transfer resonance are considered.[23] The 3.5 Å interplanar distance of solid state PBO and PBT[25] and the π-conjugated nature of their structures satisfy these requirements. The ability of these planar molecules to stack promotes formation of excited dimeric chromophores to which our photophysical observations can be attributed.

Upon photolysis, solid state samples of PBO and PBT undergo photoinduced electron transfer as shown in
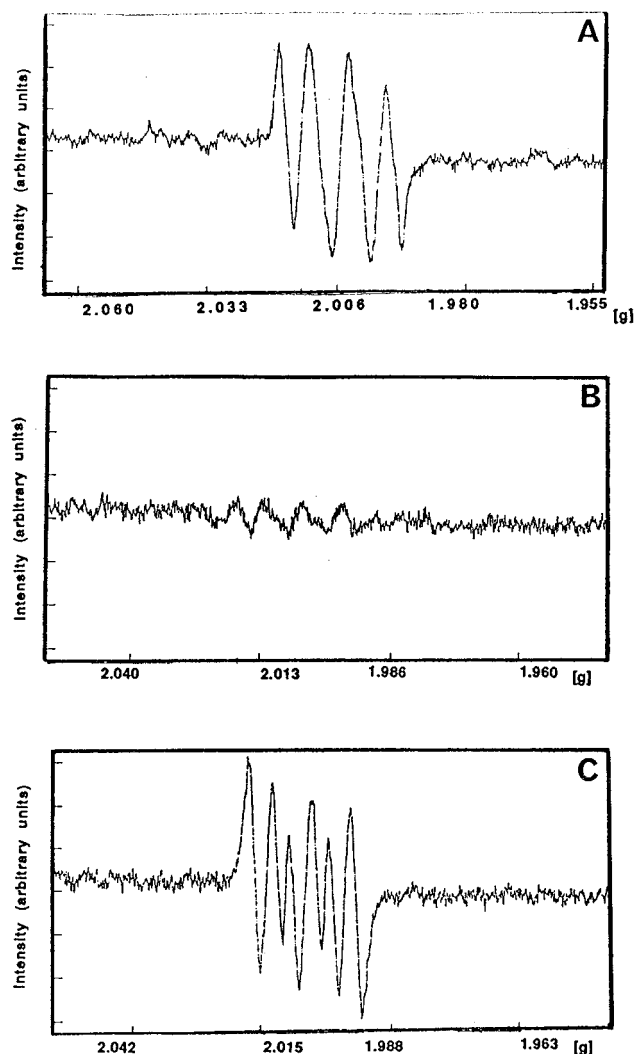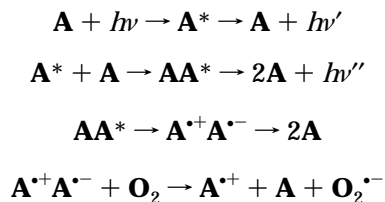
Figure 11. ESR spectra of nitrone and KO$_2$ in methanol (A), nitrone, and PBO fiber in methanol for 3 h under room light (B), nitrone and PBO fiber in methanol after 40 min exposure to UV light (C). Methanol solutions were transferred into quartz tubes for ESR experiments.

Scheme 1. In the presence of molecular oxygen, a

Scheme 1

$$\mathbf{A} + h\nu \rightarrow \mathbf{A}^* \rightarrow \mathbf{A} + h\nu'$$

$$\mathbf{A}^* + \mathbf{A} \rightarrow \mathbf{AA}^* \rightarrow 2\mathbf{A} + h\nu''$$

$$\mathbf{AA}^* \rightarrow \mathbf{A}^{\bullet+}\mathbf{A}^{\bullet-} \rightarrow 2\mathbf{A}$$

$$\mathbf{A}^{\bullet+}\mathbf{A}^{\bullet-} + \mathbf{O}_2 \rightarrow \mathbf{A}^{\bullet+} + \mathbf{A} + \mathbf{O}_2^{\bullet-}$$

superoxide radical is formed. A similar scheme was also proposed by Pickett for the photolysis of polyphenylene oxide.[19,20] Oxygen does not react with the excited benzoxazole or benzothiazole molecule effectively.

Formation of superoxide from the photolysis of PBO and PBT was detected by ESR spectroscopy using 5,5-dimethyl-1-pyrroline N-oxide (nitrone) as a radical trap. Methanol solutions of 10^{-2} M KO$_2$ and 10^{-2} M nitrone were reacted to illustrate the expected ESR signal of the hydroperoxide product, a 1:2:2:1 quartet pattern with $g = 2.0060 \pm 0.0002$ and $a^N = a^H = 15.3$G (Figure 11A).[26,27] Subsequently, 1 g of the PBO fiber was soaked in the nitrone solution for 3 h under room light prior to transferring to an ESR tube. The resulting solution
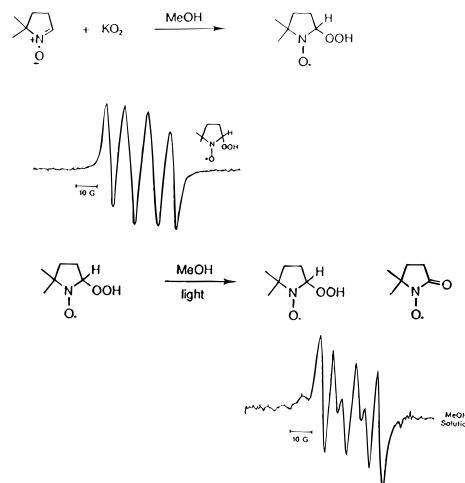

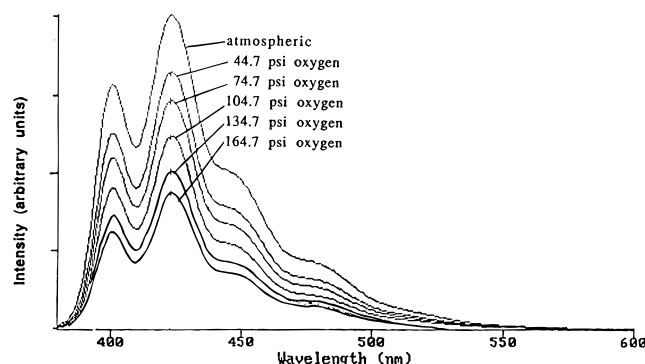**Figure 12.** Trapping superoxide by nitrone.[19,20]

Figure 13. Fluorescence spectra of **4** in toluene under high-pressure oxygen.

exhibited weak ESR signals (Figure 11B) which are superimposible with those in Figure 11A. The nitrone solution containing the PBO fiber was then irradiated with a UV source for 40 min. This solution showed strong ESR signals characteristic of the hydroperoxide product (Figure 11C) and its partial conversion to the ketonated form (Figure 12). Similar signals were also observed for PBO model compounds **4** and **9** and the PBT fiber. These experiments demonstrate that superoxide is generated during PBO and PBT photolysis in the presence of oxygen.

Strong ESR signals were also detected for PBO and PBT fibers which had been sealed in vacuum for 40 days. Similar observations have been reported by Depra and co-workers.[28,29] Oxygen was not required for the generation of these radicals.

VIII. Quenching of PBO Model Compound Fluorescence. The effects of oxygen on the fluorescence of PBO model compounds **1** and **4** in toluene was studied at external O$_2$ pressures of up to 164.7 psi.[30] Tetracyanoethylene (TCNE), a strong electron acceptor, and N,N-diethylaniline (DEA), a strong electron donor, were also used to quench the fluorescence of **1** and **4**.

A 3 × 10^{-5} M solution of **4** in toluene was placed in a high-pressure cell connected to a oxygen cylinder. After a reading was taken in air, the cell and the connection lines were flushed with oxygen. Measurements were made with oxygen pressure up to 164.7 psi.[30] The resulting fluorescence spectra are shown in Figure 13. In spite of the fact that oxygen is one of the most efficient excited state quenchers,[23] only slight quenching was observed. The data follow the normal Stern–Volmer quenching plot as shown in Figure 14.
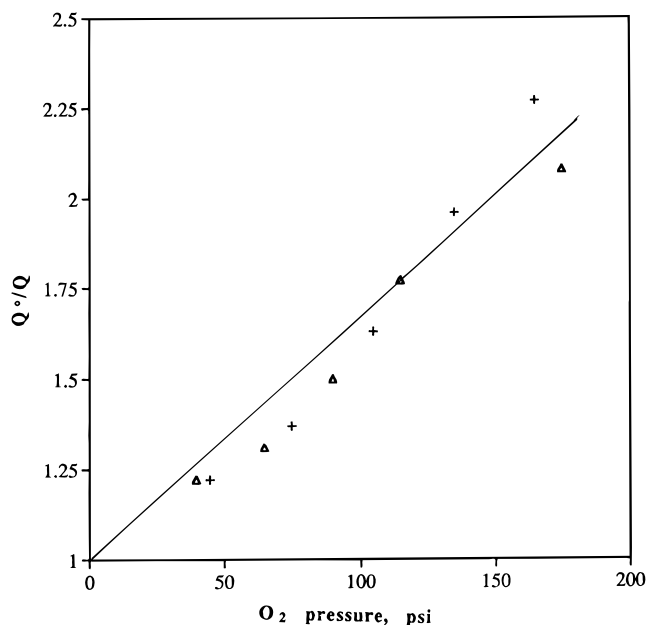
Figure 14. Stern−Volmer quenching plot of **4** by oxygen. Key: +, first experiment; ▲, second experiment.
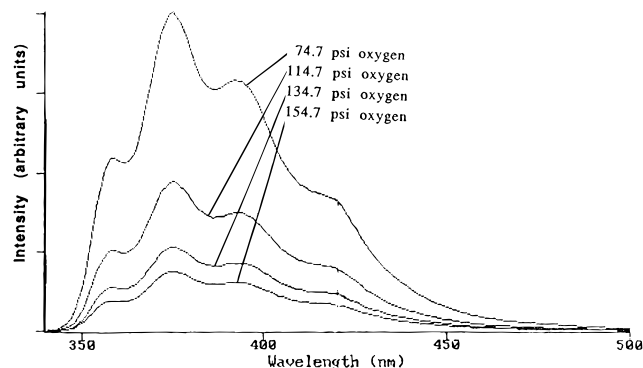

Figure 15. Fluorescence spectra of **1** in toluene under high-pressure oxygen.

The fact that the decay lifetime of **4** in solution is not noticeably affected by oxygen in air results from the slow diffusion rate of O_2 relative to the fast radiative decay rate of **4**. When [O_2] is significantly increased, quenching of fluorescence becomes detectable. Solubilities of oxygen in toluene at 34.7 psi O_2 and atmospheric air are 2.15×10^{-3} cm^3/M and 1.91×10^{-4} cm^3/M, respectively.[31]

PBO compounds including **4** in solution are photolytically stable.[9,22] The radiation quantum yield in the absence of oxygen, ϕ^0, is close to 1.[8] In the presence of oxygen, the radiation quantum yield, ϕ, is

$$\phi = k_r/(k_r + k_q[O_2])$$

where k_r is the radiative rate constant and k_q is the rate constant of quenching. Hence,

$$\phi^0/\phi = 1 + (k_q/k_r)[O_2]$$

The same experiment was performed with **1**. The results in Figure 15 show that fluorescence of **1** is quenched by oxygen efficiently at high pressures while not significantly affected by oxygen in air. In contrast to compound **4** in toluene, the data did not follow a linear Stern−Volmer quenching relationship (Figure 16). Rather, a positive deviation from linearity is
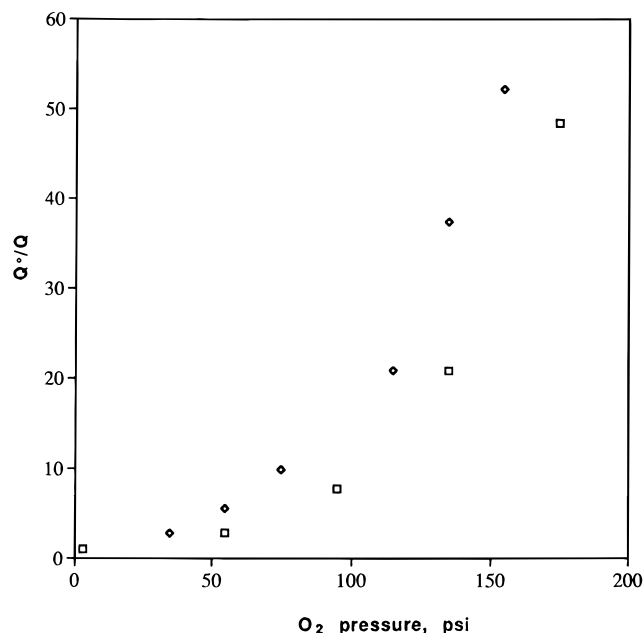

Figure 16. Stern−Volmer quenching plot of **1** by oxygen. Key: ◆, first experiment; □, second experiment.

observed, indicating enhanced quenching of the fluorescence of **1** by molecular oxygen at high pressure. In this case, the dependence on [O_2] appears quadratic in nature.

Some molecules in solution associate to form dimers at high pressure.[32,33] Due to its planar configuration, **1** has a greater tendency than **4** to form an excimer under pressure. As O_2 pressure is increased, the intermolecular distance of the excimer is expected to decrease, causing the free energy change for electron transfer formation of $A^{•+}A^{•-}$ via AA^* to be more exothermic. Therefore, the AA^* can undergo very rapid electron transfer circumventing excimer fluorescence until the electron transfer rate is retarded by the onset of the Marcus inverted region.[34]

Since photoexcited benzoxazole molecules can function as a powerful reductant in the solid state through excimer formation, the ability of these compounds to act as one-electron oxidizing or reducing agents in solution was also examined through the effects of DEA and TCNE on the fluorescence of **1** and **4**. The fluorescence of 3×10^{-5} M chloroform solutions of **1** and **4** was not quenched by either DEA or TCNE, suggesting that neither excited **1** nor **4** in solution undergo charge transfer complex formation with these strong redox active quenchers. This further supports the model shown in Scheme 1 where the short intermolecular distance of the excimer (AA^*) in the solid state is required for electron transfer formation of $A^{•+}A^-$ and the subsequent bimolecular redox chemistry with O_2.

Conclusion

Large excitation and emission energy differences are observed for benzoxazole and benzothiazole compounds and polymers in the solid state. Model compounds in solution and those with side groups which hinder the overall structural planarity show significantly smaller Stokes' shifts between the excitation and emission spectra. One emitting component is observed when a benzoxazole model compound in solution is excited. The same compound in the solid state shows two emitting species. Decay lifetimes of benzoxazole and benzothiazole compounds and polymers are not significantly

affected by the presence of oxygen in air. Quenching of the fluorescence of PBO model compounds in solution becomes detectable when the concentration of oxygen is significantly increased. For a model compound which can easily stack to form a dimer, a positive deviation from linearity in the normal Stern–Volmer plot is observed. The above data strongly suggest that intermolecular π-stacking interactions occur between planar benzoxazoles and benzothiazoles compounds leading to excimer formation *in the solid state*. In contrast, no excimer formation is detected for benzoxazole model compounds in chloroform *solution* up to 1.9×10^{-3} M under atmospheric conditions. These intermolecular π-interactions, which lead to the disparity between spectroscopic signatures for benzoxazole compounds in the solid state and in solution, are responsible for the solid state photolability of these compounds. Solid state PBO and PBT compounds undergo photoinduced electron transfer, which in the presence of molecular oxygen leads to the generation of superoxide.

Experimental Section

Material. 3,5-Di-*tert*-butylbenzoic acid, 2,3,5,6-tetramethylbenzoic acid, and 4-*n*-heptylbenzoic acid were purchased from TCI America, Chem Service, and Aldrich Chemical Co., respectively.

Synthesis of PBO Model Compounds. 2,2′-(1,4-Phenylene)bis(5-amino-6-benzoxazolol) and Its Phosphate Esters (2). To a 100 mL resin kettle equipped with a mechanical stirrer and a nitrogen inlet were added 12 g of DADHB·2HCl, 1 g of terephthalic acid, and 100 g of commercial PPA. The mixture was stirred and heated: 90 °C (4 h), 120 °C (4 h), and then 150 °C (16 h). The dope was coagulated with water, and the collected solid was washed with water in a Soxhlet extraction setup. Anal. Calcd: C, 41.58; H, 3.46; N, 9.41. Theoretical C/N ratio: 4.29. Found: 4.42. Phosphorus content was $11.5 \pm 0.6\%$ by X-ray fluorescence and $9.2 \pm 1\%$ by ^{31}P NMR. Phosphate ester ends were characterized by phosphorus-31 NMR (243 MHz, 5% NaOH/D$_2$O) δ: +2.70 (PO$_4^{-3}$), −1.84 (s, ArOPO$_3$H$_2$), −7.4 (complex[c], −PO$_2$H−), −7.5 (d, 19 Hz, −PO$_2$HPO$_3$H$_2$), −8.3 (s, PO$_3$H$_2$-PO$_3$H$_2$), −16.43 (d, 21 Hz, ArOPO$_2$H−), −17(d, 18 Hz, ArOPO$_2$H−), −17.3 (t, ArOPO$_2$H−), −22.1 (t, 19 Hz, −PO$_2$-HPO$_3$H$_2$), −22.7 (c, −PO$_2$H−), −23.1 (asymmertic t, −PO$_2$H−), −23.2 (c, −PO$_2$H−), −23.6 (c, −PO$_2$H−), −23.7 (c, −PO$_2$H−). IR (KBr): 1620 cm^{-1}. The black solid was treated with 0.1 N NaOH, and the filtrate was neutralized with concentrated HCl. One gram of product was collected. ^{1}H NMR (300 MHz, MSA) δ: 7.82 (s, 2H), 8.24 (s, 2H), 8.55 (b, 6H, −NH$_3^+$), 8.69 (s, 4H). ^{13}C NMR (75 MHz, MSA) δ: 102.12, 113.67, 120.62, 122.83, 126.62, 131.56, 151.21, 152.86, 163.52; ^{31}P NMR did not detect phosphorus. IR (KBr): 1620 cm^{-1}.

2,2′-(1,4-Phenylene)bis(6-phenylbenzo[1,2-*d*:5,4-*d*]bisoxazole (3). To a 100 mL resin kettle were loaded 1 g of **2** and 30 g of PPA. The mixture was stirred at 60 °C to make a solution. Benzoic acid (0.65 g) was added, and the following reaction procedure was used: 60 °C (6 h), 90 °C (16 h), 120 °C (4 h), and then 150 °C (5 h). Reaction product was isolated by coagulation and thoroughly washed with water. The deep brown product was dissolved in trifluoroacetic acid (TFA) and decolorized with charcoal. A yellow solid was crystallized from the TFA solution. The product was sublimed (0.1 Torr, sand bath temperature = 400 °C) to produce a yellow solid. IR (KBr): 1620 cm^{-1}. ^{1}H NMR (300 MHz, MSA) δ: 7.90–7.94 (m, 6H), 8.08–8.12 (m, 4H), 8.50 (s, 2H), 8.67 (s, 2H), 8.89 (s, 4H); ^{13}C NMR (75 MHz, MSA) δ: 101.46, 104.43, 118.91, 119.88, 126.83, 129.54, 130.24, 131.31, 131.66, 132.31, 139.87, 149.06, 149.26, 165.95, 168.70. MS *m/e*: 546, 273. Anal. Calcd for C$_{34}$H$_{18}$N$_4$O$_4$: C, 74.73; H, 3.30; N, 10.26. Found: C, 74.70; H, 3.32; N, 10.22.

2,2′-(1,4-Phenylene)bis(6-[3,5-bis(1,1-dimethylethyl)-phenyl]benzo[1,2-*d*:5,4-*d*]bisoxazole] (4). Compound **4** was prepared from **2** with 3,5-di-*tert*-butylbenzoic acid. To the

product which was slightly soluble in chloroform was added charcoal. The slurry was hot filtered. The first brown filtrate was discarded. The mixture of product and charcoal was extracted with 4% methanol in chloroform several more times. The solutions were combined, and part of the solvent was removed by evaporation. A very light yellow solid was obtained which was recrystallized in 4% methanol in chloroform. LC showed 99.7% area pure. IR (KBr): 1620 cm^{-1}. ^{1}H NMR (300 MHz, CDCl$_3$) δ: 1.44 (s, 36H), 7.64 (s 2H), 7.85 (s, 2H), 8.15 (s, 4H), 8.18 (s, 2H), 8.47 (s, 4H). MS *m/e*: 770. Anal. Calcd for C$_{50}$H$_{50}$N$_4$O$_4$: C, 77.92; H, 6.49; N, 7.27. Found: C, 77.89; H, 6.44; N, 7.32.

2,2′-(2,3,5,6-Tetramethyl-1,4-phenylene)bis(5-amino-6-benzoxazolol) (5). Compound **5** was prepared with the same procedure as **2** except that 2,3,5,6-tetramethylterephthalic acid was used instead of TA. IR (KBr): 1625, 1650 cm^{-1}. ^{13}C NMR (75 MHz, MSA) δ 17.82, 101.65, 113.76, 119.92, 121.48, 126.10, 138.07, 151.00, 152.11, 165.47.

2,2′-(2,3,5,6-Tetramethyl-1,4-phenylene)bis[6-(4-heptylphenyl)benzo[1,2-*d*:5,4-*d*]bisoxazole] (6). Compound **6** was prepared with the same procedure as **3**. The products were dissolved in chloroform and decolorized with charcoal. Two compounds were isolated by preparative TLC (silica gel, 4% methanol in chloroform). The higher spot was **6**. IR (KBr): 1620 cm^{-1}. ^{1}H NMR (300 MHz, CDCl$_3$) δ: 0.893 (t, 6H, J = 7.0 Hz), 1.34 (m, 16H), 1.68 (m, 4H), 2.18 (s, 12 H), 2.71 (t, 4H, J = 7.3 Hz), 7.37 (d, 4H, J = 8.3 Hz), 7.81 (s, 2H), 8.18 (s, 2H), 8.21 (d, 4H, J = 8.3 Hz). ^{13}C NMR (75 MHz, CDCl$_3$) δ: 14.31, 17.76, 22.87, 29.36, 29.45, 31.43, 32.01, 36.28, 93.52, 96.31, 110.39, 124.56, 127.87, 129.28, 131.15, 135.04, 139.19, 140.14, 147.51, 148.74, 149.08, 164.05, 164.34. MS *m/e*: 826. The lower spot is the higher analog. IR (KBr): 1620 cm^{-1}. ^{1}H NMR (300 MHz, CDCl$_3$) δ: 0.893 (t, 6H, J = 7.0 Hz), 1.34 (m, 16H), 1.68 (m, 4H), 2.20 (s, 24H), 2.71 (t, 4H, J = 7.3 Hz), 7.37 (d, 4H, J = 8.3 Hz), 7.82 (s, 2H), 7.88 (s, 1H), 8.18 (s, 2H), 8.21 (d, 4H, J = 8.3 Hz), 8.29 (s, 2H). MS *m/e*: 1116.

2-(4-Bromophenyl)benzoxazole (7). 4-Bromobenzoic acid (20.1 g, 0.1 mol) and *o*-aminophenol (10.9 g, 0.1 mol) were heated in 200 g of PPA at 140 °C for 3 h. The product was coagulated in water, collected, and washed thoroughly with water. The grayish product was dissolved in hot chloroform and decolorized with activated charcoal. Mp: 154–155 °C. IR (KBr) 1615 cm^{-1}. ^{1}H NMR (300 MHz, CDCl$_3$) δ: 7.34–7.41 (m, 2H), 7.57–7.61 (m, 1H), 7.76–7.81 (m, 1H), 7.68 (m, 2H), 8.13 (m, 2H). MS *m/e*: 275, 273. Anal. Calcd for C$_{13}$H$_8$-BrNO: C, 56.93; H, 2.92; N, 5.11. Found: C, 56.85; H, 2.96; N, 5.01.

Methyl 4-(2-Benzoxazolyl)benzoate. To a 250 mL pressure vessel were added **7** (12 g, 0.044 mol), bis(triphenylphosphine)palladium(II) chloride (0.288 g, 0.41 mmol), triethylamine (11.5 g, 0.114 mol), and 190 mL of methanol. The vessel was flushed four times and then sealed with CO$_2$ at 600 psi. The mixture was stirred and heated at 100 °C for 24 h and then at 110 °C for an additional 4 h. The vessel was allowed to cool to room temperature and opened. The vessel was rinsed with methylene chloride, and the palladium catalyst was removed by filtration. The methylene chloride solution was washed with water and dried with sodium sulfate. Methylene chloride was removed. The crude product was purified by column chromatography. The yield of methyl 4-(2-benzoxazolyl)benzoate was 8.0 g (0.32 mol, 73%). Mp: 180–181 °C. IR (KBr): 1720 cm^{-1}. ^{1}H NMR (300 MHz, CDCl$_3$) δ: 3.67 (s, 3H), 7.37–7.40 (m, 2H), 7.59–7.62 (m, 1H), 7.79–7.82 (m, 1H), 8.18–8.21 (m, 2H), 8.32–8.35 (m, 2H). MS *m/e*: 253, 238, 222, 194. Anal. Calcd for C$_{15}$H$_{11}$NO$_3$: C, 71.15; H, 4.35; N, 5.53. Found: C, 71.10; H, 4.38; N, 5.50.

Unreacted **7** (1.6 g) was recovered.

4-(2-Benzoxazolyl)benzoic Acid (8). Methyl 4-(2-benzoxazolyl)benzoate (10.1 g, 0.04 mol) was stirred in 250 mL of a 3:1 mixture of methanol and water with 8 g of NaOH at room temperature overnight. The mixture was cooled with ice and neutralized with HCl. A white solid was collected, washed with water, and dried. Yield: 9.0 g (94%). Mp: 192–194 °C. IR (KBr): 3061, 2999, 2881, 2673, 2553, 1618 cm^{-1}. ^{1}H NMR (300 MHz, DMSO-d_6) δ: 7.40–7.44 (m, 2H), 7.69–7.81 (m, 2H),

8.14−8.32 (m, 4H). ^{13}C NMR (75 MHz, DMSO-d_6) δ: 109.1, 118.4, 123.1, 124.0, 125.5, 128.3, 128.5, 131.9, 140.0, 148.8, 159.8, 165.0. MS m/e: 239, 194. Anal. Calcd for $C_{14}H_9NO_3$: C, 70.29; H, 3.77; N, 5.86. Found: C, 70.38; H, 3.80; N, 5.81. Compound **8** was also prepared from the Grignard reagent of **7** and CO_2 or with a similar procedure for the synthesis of 4-(2-benzothiazolyl)benzoic acid described below.

2,6-Bis[4-(2-benzoxazolyl)phenyl]benzo[1,2-*d*:5,4-*d*′]-bisoxazole (9). To a 100 mL resin kettle equipped with a mechanical stirrer and a nitrogen inlet were added 4-benzoxazolylbenzoic acid (941.2 mg, 4.94 mM), DADHB·2HCl (420 mg, 1.97 mM), and PPA (43 g). The mixture was stirred at 70 °C (1 h), 90 °C (2 h), 110 °C (16 h), and 140 °C (24 h). An aliquot was coagulated in ice−water, and IR analysis of the solid showed unreacted carboxylic acid remaining.[35] DADHB·2HCl (50 mg) was added, and the mixture was stirred at 140 °C for another 24 h. Another aliquot was removed and coagulated with ice−water. IR analysis of the product showed complete disappearance of carboxylic acid. A brownish solid (1.0 g) was obtained when the coagulated product was thoroughly washed with water and dried to constant weight. The solid was dissolved in 30 mL of TFA with warming. A yellow solid precipitated after some TFA was removed by evaporation. The yellow solid was collected in a sintered glass filter and washed with water and then chloroform. The yellow solid was recrystallized in TFA. A light yellow solid was collected in a 60 mL sintered glass filter, and water was put into the crucible to remove TFA. The washing procedure was repeated at least 20 times. The lump-shaped solid was dried in a vacuum oven at 100 °C for 4 h. IR (KBr): 1620 cm^{-1}. ^{1}H NMR (300 MHz, MSA-d_4) δ: 7.93 (m, 4H), 8.10 (m, 4H), 8.77 (d, 4H, J = 13 Hz), 8.82 (d, 4H, J = 13 Hz), 8.85 (s, 1H), 8.95 (s, 1H). ^{13}C NMR (75 MHz, MSA) δ: 101.88, 105.90, 114.59, 117.20, 125.96, 127.85, 129.37, 130.18, 130.76, 131.79, 132.41, 149.59, 150.38, 162.61, 166.68. Although C-13 NMR spectrum did not show residual TFA, the fluorine-19 NMR spectrum showed an estimation of 0.1−0.5 molecules of TFA per PBO model molecule. The estimation was based on comparison with the signals in a F-19 NMR spectrum obtained by adding a known amount of TFA to a NMR tube with the same volume of MSA. Compound **9** was purified by sublimation at 350 °C/0.2 mmHg. MS m/e: 546. Anal. Calcd for $C_{34}H_{18}N_4O_4$: C, 74.73; H, 3.30; N, 10.26. Found: C, 74.76; H, 3.31; N, 10.32.

4-(2-Benzothiazolyl)benzonitrile (10). 4-Cyanobenzoyl chloride (25 g) in 50 mL of chloroform was added dropwise to a solution of *o*-aminothiophenol (18.9 g) and triethylamine (15.3 g) in 100 mL of chloroform at room temperature. After the addition was complete, the solution was refluxed for 2 h. The solid obtained after solvent removal was washed with water, dried, and heated at 250 °C under vacuum generated by an aspirator. Pure **10** was isolated by a silica gel column packed with a 20:80 mixture of ethyl acetate and hexane. Mp: 164−166 °C. IR (KBr): 2230 cm^{-1}. ^{1}H NMR (300 MHz, CDCl$_3$) δ: 7.49 (m, 2H), 7.75 (d, 2H, J = 8.0 Hz), 8.01 (m 2H) 8.18 (d, 2H, J = 8.0 Hz). ^{13}C NMR (75 MHz, CDCl$_3$) δ: 114.08, 118.16, 121.71, 123.75, 126.00, 127.84, 132.65, 135.26, 137.42, 153.97, 165.22. MS m/e: 236. Anal. Calcd for $C_{14}H_8N_2S$: C, 71.19; H, 3.39; N, 11.86. Found: C, 71.10; H, 3.44; N, 11.64.

4-(2-Benzothiazolyl)benzoic Acid (11). One gram of **10** was dissolved in 150 mL of a 2:1 mixture of water and MSA. The yellow solution was stirred at 100 °C for 20 h and then was poured into ice−water. The solid was collected and washed with water. NaOH solution (0.1 N) was used to dissolve the acid. The solution was filtered, and the filtrate was neutralized with concentrated HCl to precipitate the white product (0.9 g). MS m/e: 255. IR (KBr): 1680 cm^{-1}. ^{1}H NMR (300 MHz, DMSO-d_6) δ: 7.55 (m, 2H), 8.15 (m, 6H). ^{13}C NMR (DMSO-d_6) δ 122.37, 123.11, 125.86, 126.76, 127.23, 130.16, 132.88, 134.66, 136.33, 153.44, 166.04, 166.53. Anal. Calcd for $C_{14}H_9NO_2S$: C, 65.88; H, 3.53; N, 5.49. Found: C, 65.93; H, 3.48; N, 5.44.

2,6-Bis[4-(2-benzothiazolyl)phenyl]benzo[1,2-*d*:4,5-*d*′]-bisthiazole (12). To a 100 mL resin kettle were loaded 0.4717 g of **11**, 0.2283 g of DADTB·2HCl, and 47 g of PPA. The mixture was stirred and heated at 70 °C (2 h), 90 °C (2 h), 135 °C (6 h), and then 180 °C (16 h). The product was

coagulated, collected, and washed thoroughly with water. The yellow product was crystallized in TFA. The sample was purified by sublimation at 0.1 Torr with a sand bath at 400 °C. IR (KBr): 1530, 1550 cm^{-1}. ^{1}H NMR (300 MHz, MSA-d_4) δ: 7.85 (m, 4H), 8.10 (m, 4H), 8.60 (m, 8H), 9.30 (s, 2H). ^{13}C NMR (75 MHz, MSA) δ: 114.84, 118.47, 124.36, 130.20, 130.23, 130.60, 131.10, 131.17, 131.50, 131.96, 133.06, 140.10, 140.87, 171.58, 177.21. MS m/e: 610, 305. Anal. Calcd for $C_{34}H_{18}N_4S_4$: C, 66.89; H, 2.95; N, 9.18. Found: C, 66.93; H, 2.30; N, 9.10.

2,6-Bis(4-*tert*-butylphenyl)benzo[1,2-*d*:4,5-*d*′]bisoxazole (13). ^{1}H NMR (300 MHz, CDCl$_3$) δ: 1.42 (s, 18H), 7.59 (d, 4H, J = 8 Hz), 7.80 (s, 1H), 8.12 (s, 1H), 8.23 (d, 4H, J = 8 Hz). ^{1}H NMR (300 MHz, MSA-d_4) δ: 1.40 (s, 18H), 7.90 (d, 4H, J = 7 Hz), 8.36 (d, 4H, J = 7 Hz), 8.43 (s, 1H), 8.67 (s, 1H). ^{13}C NMR (75 MHz, CDCl$_3$) δ: 31.07, 35.02, 93.03, 109.44, 124.13, 125.86, 127.30, 139.83, 148.61, 155.14, 163.78. ^{13}C NMR (75 MHz, MSA) δ: 31.53, 37.28, 101.41, 103.50, 116.99, 129.23, 129.85, 131.58, 148.95, 165.20, 168.35.

Fiber Preparation. PBO Fiber. PBO polymer and fiber were produced by The Dow Chemical Co. The following was the procedure for mixing, dehydrohalogenation, oligomerization, and molecular weight buildup.[36] A 100 lb quantity of PPA containing 83.7 wt % P_2O_5 was added to a 25 gallon reactor with agitation by a helical dual ribbon impeller. At 60 °C under nitrogen atmosphere, 19.01 lbs of DADHB, 14.38 lbs of micronized TA, and 21.99 lbs of P_2O_5 were added. Mixing was continued for 1 h at 60 °C and about 6 h at 120 °C. Hydrogen chloride gas evolved was drawn off and recovered. The reaction temperature was raised to 140 °C, until a viscosity of about 300 poise was reached. The resulting solution was pumped into a tank and stored under nitrogen atmosphere at about 120 °C.

The reaction mixture was pumped through a twin screw extruder having about a 35:1 length to diameter ratio and an internal diameter of about 30 mm. The temperature was between 190 and 210 °C. The residence time was about 6 min. The flow through the extruder was about 10 lb of dope per h. The extruder has a syringe pump that could introduce a measured flow of liquid into the extruder. A mixture of 10 wt % TA in PPA was introduced. The dope leaving the extruder passed through a series of four static mixing elements. The effect of the TA as the chain extender on the dope was controlled by monitoring the pressure drop across the mixers. The resulting polymer had viscosity of 30 dL/g. Polymer viscosity was also measured by dissolving some of the isolated polymer in MSA at 25 °C and a concentration of 0.05 g/dL.

PBO fiber was spun from the dope.[4,37] The polymer solution was mixed and degassed with a twin screw extruder at 170 °C. The dope was extruded from the spinneret having 166 holes. The capillary diameter of the holes was 0.22 mm. The spin draw ratio was 63. The extruded yarn was introduced into a coagulation bath which has a spinning funnel installed 55 cm below from the spinneret and in which coagulation water was maintained at about 22 °C. The fiber was washed to remove residual acid, and moisture in the fiber was removed by contacting on a heating roller. PBO fiber used in the experiments were not heat treated. Tensile strength and tensile modulus of the as spun fiber were 750 ksi (5.17 GPa) and 31 Msi (214 GPa), respectively.

PBT Fiber. A mixture containing 245 g of DADTB, 166 g of micronized TA, 1527 g of 83.5% PPA, and 365 g of P_2O_5 was agitated under nitrogen using a mechanical stirrer at 70 °C for 2 h, 120 °C for 4 h, and 150 °C for 2 h. Most of the mixture was transferred to a piston-agitated reactor and heated at 210 °C for 3 h to complete the reaction. The dope was extruded from a spinneret having 36 holes. The capillary diameter of the holes was 0.22 mm. The spin draw ratio was 50. The extruded yarn was introduced into a coagulation bath which has a spinning funnel installed 10 cm below the spinneret and in which coagulation water was maintained at about 22 °C. The fiber was washed to remove residual acid, and moisture in the fiber was removed by contacting on a heating roller.

PBT fiber used in the experiments were not heat treated. Intrinsic viscosity of the polymer was 36 dL/g. The tensile strength and tensile modulus of the as spun PBT fiber were

400 ksi (2.76 GPa) and 28 Msi (193 GPa), respectively. After heat treatment at 600 °C for 10 s in a tube furnace under nitrogen, tensile strength and tensile modulus were 380 ksi (2.62 GPa) and 40 Msi (276 GPa). A heat-treated PBT fiber sample prepared by duPont had tensile strength of 280 ksi (1.93 GPa) and tensile modulus of 39 Msi (269 GPa).

Absorption Spectroscopy. Absorption spectra were collected using a Cary UV−vis absorption spectrometer system (Model 2400, Varian Instrument Group).

Fluorescence Spectroscopy. All fluorescence excitation and emission spectra were collected with a Spex Fluorlog 2 system equipped DM3000 software (Spex Industries, Edison, NJ 08820). Samples were illuminated with a 150 W xenon arc lamp operating at a current of 25 amps. Excitation and emission wavelengths were determined using two 0.22 m double monochromators (Spex Industries, Model 1680), and spectral bandpass values for the excitation of and the observed emission by the sample were 5 and 1 nm, respectively. Spectra were collected employing either front face or right angle geometry with a scanning rate of 1 nm/s and were collected in a manner to compensate for fluctuations in the xenon arc excitation source. Following acquisition, all data were transferred to a minicomputer (IBM AT), analyzed, and plotted using Spectra Calc software routines.

Solid state samples were prepared by sandwiching the powder or fiber between two thin quartz plates. The assembled "sandwich" was placed within a standard 1 cm × 1 cm quartz cuvette and positioned such that the glass plate was flush against the inside wall of the cuvette. Spectra were then acquired using front face geometry.

Fluorescence spectra of PBO and PBT compounds in solution were collected using 10 mm quartz cuvettes. Both front face and right angle collection geometries were utilized as dictated by the type of experiment.

For high-pressure experiments, a stainless steel cell with a quartz window and a 1 in. diameter cylindrical cavity was used. A metal gas line was connected to the top of the cell. Oxygen pressure was measured with a pressure gauge. Numbers reported in this article are in absolute pressure. After oxygen was increased to a certain reading, the cell was shaken several times until a constant fluorescence intensity value was recorded. Experiments were performed at front face.

Lifetime Decay Measurements. Solid samples were placed in 5 mm diameter quartz tubes. Some of these tubes were then sealed under vacuum at 10^{-3} Torr. Compounds **1** and **4** were dissolved in toluene to form 5×10^{-6} M solutions. Portions of the solutions were evacuated by several freeze and thaw cycles.

Luminescence lifetime measurements were made utilizing instrumentation housed in the LASER (Laser Applications in Science and Engineering Research) Laboratory at Michigan State University. The time-correlated single photon counting instrument has been described elsewhere.[38] Luminescence decays were obtained between 450 and 650 nm following sample excitation at 290 nm with the frequency doubled output of the Coherent 702 dye laser operation at 580 nm (6 ps FWHM) and repetition rates of 2 MHz. Solution samples were prepared in 1 cm quartz cuvettes and degassed as denoted in the text.

ESR Spectroscopy. ESR measurements were performed on a Bruker X-band ESP 300e spectrometer, serial number ZG756, which operates at frequency of 9.4 GHz. The ESR spectra were recorded in the first derivative mode using a modulation frequency of 100 kHz. The modulation amplitude was kept small compared to the ESR line width to avoid any line shape distortion. The spectrometer frequency was measured to an accuracy of ± 1 kHz with the aid of a microwave frequency counter, EIP Model 625A. The spectrometer is also equipped with an NMR Gaussmeter, Model ER035M-IEC, located very close to the center of the ESR cavity and capable of measuring the magnetic field to the nearest 0.01 G. A variable-temperature accurate to ± 1 °C unit was used to control and measure the temperature of the sample. The *g*-value of the ESR spectrum was calculated from the measured magnetic field and frequency at resonance.

PBO and PBT fiber samples sealed in vacuo for lifetime decay measurements were used for the ESR experiments. Fiber and model compound samples in nitrone methanol solution were photolyzed 6 in. away from a 450 W medium mercury arc lamp purchased from Ace Glassware. Fiber and model compound samples were removed by filtration, and the solutions were placed in quartz tubes for ESR experiments.

References and Notes

(1) Wolfe, J. F. In *Encyclopedia of Polymer Science and Technology*, 2nd ed.; Mark, H. F., Kroschmitz, J. I., Eds.; Wiley: New York, 1988; Vol. 11, pp 601−635.

(2) *The Materials Science and Engineering of Rigid-Rod Polymers*; Adams, W. W., Edy, R. K., McLemore, D. E., Eds.; Symposium Proceedings; Vol. 134. Materials Research Society: Pittsburgh, 1989.

(3) Yang, H. H. *Aromatic High-Strength Fibers*; Wiley-Interscience: New York, 1989; Chapter 2.

(4) Rosenberg, S.; Quarderer, G. J., Jr.; Sen, A.; Nakagawa, M.; Faley, T. L.; Serrano, M.; Teramoto, Y.; Chau, C. C. U.S. Patent 5,294,390, 1994.

(5) Yang, H. H. *Aromatic High-Strength Fibers*; Wiley-Interscience: New York, 1989; p 248.

(6) Uy, W. C.; Mammone, J. F. *Abstracts of Papers*; 189th National Meeting of the American Chemical Society, Miami, FL; American Chemical Society: Washington, DC, 1985; Cellulose, Paper and Textile Fibers Division 11.

(7) PBO fiber is being commercialized by Toyobo Co., Japan.

(8) Reiser, A.; Leyshon, L. J.; Saunders, D.; Mijovic, M. V.; Bright, A.; Bogie, J. *J. Am. Chem. Soc.* **1972**, *94*, 2414−2425.

(9) Gusten, H.; Rinke, M.; Kao, C.; Zhou, Y.; Wang, M.; Pan, J. *Opt. Commun.* **1986**, *59*, 379−384.

(10) (a) Osaheni, J. A.; Jenekhe, S. A. *Macromolecules* **1994**, *27*, 739−742. (b) Jenekhe, S. A.; Osaheni, J. A. *Science* **1994**, *265*, 765−768.

(11) (a) Jenekhe, S. A.; Osaheni, J. A. *Chem. Mater.* **1994**, *6*, 1906−1909. (b) Osaheni, J. A.; Jenekhe, S. A. *J. Am. Chem. Soc.* **1995**, *117*, 7389−7398.

(12) (a) Lefkowitz, S. M.; Roitman, D. B. *Polymer* **1994**, *35*, 1576−1579. (b) Leugers, M. A.; Lefkowitz *Polymer* **1994**, *35*, 4235−4237.

(13) Reinhard, Z.; Heinz, H. In *Encyclopedia of Chemical Technology*, 3rd ed.; Grayson M., Ed.; Wiley: New York, 1978; Vol. 4, pp 213−226.

(14) Fouassier, J. P.; Lougnot, D. J.; Wieder, F.; Faure, J. *J. Photochem.* **1977**, *7*, 17−28.

(15) Fletcher, A. N.; Henry, R. A.; Kubin, R. F.; Hollins, R. A. *Opt. Commun.* **1984**, *48*, 352−356.

(16) Dollish, F. R.; Fateley, W. G.; Bentley, F. F. In *Characteristic Raman Frequencies of Organic Compounds*; Wiley: New York, 1974; pp 162−241.

(17) Alder, R. W.; Baker, R.; Brown, J. M. *Mechanism in Organic Chemistry*; Wiley-Interscience: London, 1971; pp 24−26.

(18) Gugumus, F. In *Oxidation Inhibition in Organic Materials*; Pospisil, J., Klemchuk, P. P., Eds.; CRC Press: Boca Raton, 1990; Vol. II, pp 29−162.

(19) Pickett, J. E. In *Polymer Stabilitization and Degradation*; ACS symposium Series 280; American Chemical Society: Washington, DC, 1985; pp 313−328.

(20) Pickett, J. E. In *Mechanism of Polymer Degradation and Stabilization*; Scott, G., Ed.; Elservier: Amsterdam, 1990; pp 135−167.

(21) Rabek, J. F.; Sanetra, J.; Ranby, B. *Macromolecules* **1986**, *19*, 1674−1679.

(22) So, Y. H.; Bell, B.; Pfeiffer, C.; Leflowitz, S.; Murlick, C. L.; Martin, S. To be published.

(23) Barltrop, J. A.; Coyle, J. D. *Excited States in Organic Chemistry*; Wiley & Sons: London, 1975; pp 101−132.

(24) The fluorescence of **1** in chloroform at the front face was measured. The intensities at 373 nm of 1×10^{-4} M, 6.4×10^{-4} M, and 1.9×10^{-3} M were 3.3×10^7, 3.4×10^7, and 3.54×10^7, respectively.

(25) Fratini, A. V.; Lenhert, P. G.; Resch, T. J.; Adams, W. W. In *The Materials Science and Engineering of Rigid-Rod Polymers*; Adams, W. W., Edy, R. K., McLemore, D. E., Eds.;

Symposium Proceedings, Vol. 134; Materials Research Society: Pittsburgh, 1989; pp 431−445.

(26) Harbour, J. R.; Chow, V.; Bolton, J. R. *Can. J. Chem.* **1974**, *52*, 3549−3553.

(27) Harbour, J. R.; Bolton, J. R. *Biochem. Biophys. Res. Commun.* **1975**, *64*, 803−807.

(28) (a) Depra, P. A.; Gaudiello, J. G.; Marks, T. J. *Macromolecules* **1988**, *21*, 2295−2297. (b) Depra, P. A. Ph.D. Thesis, Northwestern University, June 1989.

(29) PBO and PBT fiber described in this paper were not heat treated unless specified. Strong ESR signals identical to those observed for as spun fibers were also observed for heat-treated PBO and PBT fiber prepared at Dow and a heat-treated PBT fiber sample prepared by duPont. ESR experiments for heat-treated fibers were performed in air only.

(30) Numbers are absolute pressures which are gauge pressures plus 14.7 psi.

(31) The solubility of oxygen in toluene at 298.15 K and 1 atm partial pressure is 9.09×10^{-4}. The numbers are calculated with Henry's Law: $(9.09 \times 10^{-4})(34.7/14.7) = 2.15 \times 10^{-3}$ and $(9.09 \times 10^{-4})(21/100) = 1.91 \times 10^{-4}$. Wilhelm, E.; Battino, R. *Chem. Rev.* **1973**, *73*, 1−9.

(32) Roberts, E. R.; Drickamer, H. G. *J. Phys. Chem.* **1985**, *89*, 3092−3095.

(33) Taguchi, T.; Hirayama, S.; Okamoto, M. *Chem. Phys. Lett.* **1994**, *231*, 561−568.

(34) *Photoinduced Electron Transfer* I; Mattay, J., Ed.; Topics in Current Chemistry 156; Springer-Verlag: New York, 1990.

(35) For unclear reasons, excess DADHB is required to completely convert the carboxylic acid to benzoxazole. This is not true for **12**, a similar PBT model compound.

(36) Gregory, T.; Hurtig, C. W.; Ledbetter, H. D.; Quackenbush, K. J.; Rosenberg, S.; So, Y. H. U. S. Patent 5,194,568, 1993.

(37) Chau, C. C.; Faley, T. L.; Mills, M. E.; Nakagawa, M.; Rehg, T. J.; Serrano, M.; Shanker, R.; Quarderer, G. J.; Teramoto, Y. U. S. Patent 5,296,185, 1994.

(38) Bowman, L. E.; Berglund, K. A.; Nocera, D. G. *Rev. Sci. Inst.* **1993**, *64*, 338.